Applicability of evolutionary algorithms for orbit optimization in the strongly perturbed environment of the 2001 SN263 triple asteroid system

Obrecht, Guillaume; Cowan, Kevin; de Almeida Prado, Antonio Fernando

Publication date
2020

Document Version
Final published version

Published in
Proceedings of the 2nd IAA/AAS SciTech Forum 2019 (SciTech Forum on Space Flight Mechanics and Space Structures and Materials), Moscow, Russia, 25 June 2019

Citation (APA)
Obrecht, G., Cowan, K., & de Almeida Prado, A. F. (2020). Applicability of evolutionary algorithms for orbit optimization in the strongly perturbed environment of the 2001 SN263 triple asteroid system. In B. W. Hansen (Ed.), *Proceedings of the 2nd IAA/AAS SciTech Forum 2019 (SciTech Forum on Space Flight Mechanics and Space Structures and Materials), Moscow, Russia, 25 June 2019* (Vol. 174, pp. 205-225). Article AAS 19-965 AAS/AIAA.

Important note
To cite this publication, please use the final published version (if applicable).
Please check the document version above.

IAA-AAS-SciTech2019-013
AAS 19-965

APPLICABILITY OF EVOLUTIONARY ALGORITHMS FOR ORBIT OPTIMIZATION IN THE STRONGLY PERTURBED ENVIRONMENT OF THE 2001 SN263 TRIPLE ASTEROID SYSTEM

Guillaume Obrecht,[*] Kevin Cowan[†] and Antonio F. B. A. Prado[‡]

The ASTER mission under study by the Brazilian National Institute for Space Research would be the first to explore a triple asteroid system. To find orbits stable in such a perturbed environment, an orbit propagation and optimization programme has been written, which makes use of Evolutionary evolution algorithms. The programme written proves sufficient to identify suitable solutions for several use cases based on various mission phases and scenarios. The solar radiation pressure has been identified as a critical perturbation that prevents the existence of solutions in some scenarios, and often drives existing solutions towards terminator orbits.

INTRODUCTION

Aster is the first Brazilian mission to an asteroid. Its target is the (153591) 2001 SN263 asteroid system. It has been first observed in 2001 by the LINEAR (Lincoln Near-Earth Asteroid Research) project and confirmed to be a triple system in 2008 by the Arecibo Observatory in Puerto Rico.[1] It has an Amor class orbit, which means it approaches, without crossing, the orbit of the Earth, and crosses the orbit of Mars.[2] The main motivation for this mission is the development of the technology and knowledge of the Brazilian space sector.[3]

The scientific objectives of Aster have been defined as follows:[4] the main measurements to be made include the bulk properties (size, shape, mass, density, dynamics, spin state), the internal properties (structure, gravity field) and the surface properties (mineralogy, morphology, elemental composition).

The spacecraft under study for this mission is based on the Russian low-cost MetNet platform, with an initial mass of 152 kg including 30 kg dedicated to the payload and a nominal power of 2.1 kW.[3] This platform relies on low thrust engines,[5] for propulsion, manoeuvres and attitude control. The payload of the spacecraft[1] is composed of a multi-spectral camera, a laser rangefinder (ALR), a near infrared spectrometer and a mass spectrometer.

This study looks at the exploration phase of the mission, which requires a parking orbit for the spacecraft upon arrival in the system, and one or several exploration orbits to study the three bodies of the system. Two schemes are considered:[6] a *sequential exploration*, each body requiring a different orbit for its study, or a *parallel exploration* in which the spacecraft is inserted into an elliptical

[*] CS Communications and Systems GmbH, 64295 Darmstadt, Germany.
[†] Faculty of Aerospace Engineering, Delft University of Technology, 2629 HS Delft, The Netherlands.
[‡] National Institute for Space Research, 12227-010 São José dos Campos, Brazil.

orbit crossing the orbits of all bodies. This study aims at answering the following question: What kinds of orbits are suitable for the exploration phase of the ASTER mission? What is the best strategy to explore the three bodies of the 2001 SN263 asteroid system? How efficient are Evolutionary Algorithms at finding optimal orbits in the complex and highly perturbed environment of the 2001 SN263 triple asteroid system?

PROBLEM GEOMETRY AND ASSUMPTIONS

This section presents the problem properties and the assumptions made to represent its geometry and the forces ruling it.

Asteroid system geometry

Due to the large distance of the asteroid system from the Earth and the imprecision on the measurements, little is known on the actual motions of the asteroids until the spacecraft approaches the asteroid system. Its physical properties as well as orbital elements were determined through a detailed study based on best model fits for the orbits and 1σ statistical errors analysis.[7] Many parameters (masses, J_2 effect and orbital parameters) have a relatively big formal statistical error. The choice has been made to fix all parameters as the best fit values,[7] summarised in Table 1.

Table 1: Properties and orbital elements of the triple asteroid 2001 SN263 (at epoch MJD 54509)

		Alpha (central body)	Beta (outer)	Gamma (inner)
Orbits		Sun	Alpha	Alpha
Mass		917.466×10^{10} kg	24.039×10^{10} kg	9.773×10^{10} kg
Radius		$\approx$1.3 km	$\approx 0.39\,\mathrm{km}$	$\approx 0.29\,\mathrm{km}$
2^{nd} dynamic form factor	J_2	0.013	Unknown	Unknown
Semi-major axis	a	1.99 ua	16.633 km	3.804 km
Eccentricity	e	0.48	0.015	0.016
Inclination	i	6.7°	0° (by convention)	14°
Period	P	2.80 y	6.225 d	0.686 d

An inertial reference frame (O, x, y, z) is defined as centred on the centre of the asteroid system O, which is, in the simplified model considered, the centre of mass of Alpha. The x and y axis are defined to be in the ecliptic, with x pointing toward the Sun, hence z is the normal to the ecliptic. Given this inertial reference frame, the asteroid system is represented by the model as follows, and shown in Figure 1:

- The body Alpha is fixed on the origin O of the reference frame;
- The Sun is placed on the x axis, at a positive distance to be chosen between the perihelion and aphelion of the asteroid system (respectively 1.04 ua and 2.94 ua);
- The orbital plane of Beta is placed, by convention, in the (O, x, y) plane;
- As a consequence, the orbital plane of Gamma makes a 14° angle with the orbital plane of Beta;

- The direction of the Sun $(+x)$ being the reference direction, the longitude of the ascending node for the orbit of Gamma is arbitrarily chosen to be $0°$.

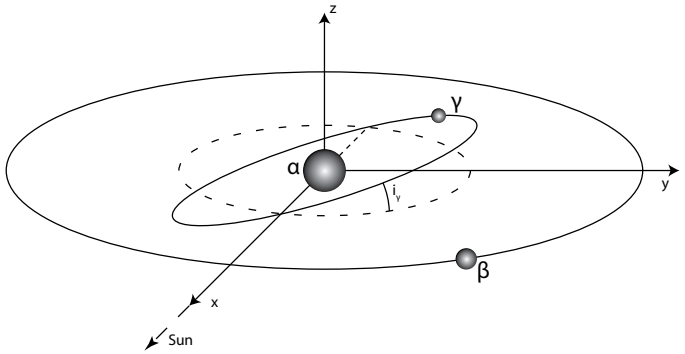

Figure 1: Geometry adopted to represent the 2001 SN263 asteroid system.

Force modelling

Gravitational attraction. The motion of a spacecraft within this triple asteroid system is guided by a four-body problem. The problem is also restricted, with the mass of the spacecraft considered to be negligible with respect to the primaries, Alpha, Beta and Gamma. The four-body problem has no analytical solutions like the two-body problem, and no interesting or generalisable properties like the three-body problem. Typical four-body problems studied in the literature, such as the *bicircular restricted model*[8,9] (used for the Sun-Earth-Moon system) or the *concentric circular restricted model*[9,10] (used for the Jupiter-Ganymede-Callisto system) are not applicable for this asteroid system because of major differences in the geometry. The system could be assimilated with a concentric circular restricted model, but there is a difference of $14°$ between the inclination of the two moon's orbital planes, and the masses of Beta and Gamma are not negligible compared with the mass of Alpha (respectively only 40 and 94 times lighter).

The motion of a spacecraft in the asteroid system is hence obtained through a numerical integration in which at each step the exact contributions of each force are calculated and added, and then used to compute the acceleration of the spacecraft and integrate its next state. Some simplifications were done on the motion of the primaries. They are motivated by a previous study[7] which concluded that the orbits of Beta and Gamma match quite well Keplerian orbits about Alpha, with precession rates relatively small compared to the integration times considered: typically less than $0.1\,^\circ\,\mathrm{d}^{-1}$ for Beta and less than $2.5\,^\circ\,\mathrm{d}^{-1}$ for Gamma.

Another very strong hypothesis is to place Alpha at the origin of the system (i.e., the centre of the reference frame), while it should have its own orbit around the barycentre of the system under the influence of Beta and Gamma. However, in the worst case the offset between the barycentre of the system and the centre of mass of Alpha is 0.483 m, to be put into perspective with the uncertainties on the orbital parameters and physical properties of the bodies.[7] For instance, the mass of Beta, which is the main element driving the offset between the centre of mass of Alpha and the barycentre, can be expected to be anywhere between 7.039×10^{10} kg and 31.039×10^{10} kg. The uncertainty on the semi-major axis of Beta is 770 m, which is larger than the maximum offset of Alpha. This assumption is hence considered as reasonable for this study. Nevertheless, it introduces a small

inconsistency: the fact that Beta and Gamma are on Keplerian orbits, as well as the use of the central gravity acceleration models, imply that the reference frame used is inertial and centred on the barycentre of the system; on the contrary, the fact that Alpha is fixed at the origin of the system would imply that the reference frame is centred on Alpha, and hence quasi-inertial.

The model used to represent the problem is defined as follows: the main primary Alpha is fixed at the origin of the system, Beta is in a purely Keplerian motion about Alpha, Gamma is in a purely Keplerian motion about Alpha. Alpha, Beta and Gamma are considered as point-masses, and the spacecraft is, at any moment, undergoing a gravitational attraction from Alpha, Beta and Gamma (under Newton's law of gravitation).

The gravitational attraction undergone by the spacecraft from Alpha, Beta and Gamma is computed individually. This force uses the central gravity acceleration model. The acceleration of the spacecraft due to the gravitational attraction of a body i is given by:

$$\mathbf{a}_{g_i} = G\frac{m_i}{r_i^2}\mathbf{e}_i \tag{1}$$

Solar radiation pressure. The solar radiation pressure is computed using a cannonball radiation pressure force model, *i.e.* the resulting force will be entirely in the anti-Sun direction. Its expression is as follows:[11]

$$\mathbf{a}_{SRP} = -C_R\frac{W \cdot A}{m_{S/C} \cdot c}\mathbf{e}_S \tag{2}$$

The power density of the incoming radiation W is obtained from the power density of the incoming radiation at the Earth * $W_{1\,\mathrm{ua}} = 1361\,\mathrm{W\,m^{-2}} : W = \frac{1\,\mathrm{ua}}{d}W_{1\,\mathrm{ua}}$. The radiation pressure coefficient C_R depends on the reflection characteristics of the materials of the spacecraft. Although the exact shape and size of the spacecraft has not been decided yet, informal discussions with people working on the ASTER mission led to consider a cross section area of $20\,\mathrm{m^2}$ and a radiation pressure coefficient of 1.21, typical for solar panels.[12] In this study, the solar radiation pressure force model does not consider the occlusion of the Sun by bodies.

Neglected perturbations. The gravity field perturbations might have a non-negligible effect on the motion of a spacecraft, due to the usually very irregular shape of asteroids. Nevertheless, the shape of the asteroids is a great unknown of the problem which will only be resolved upon arrival of the spacecraft at the system. At most the current studies give a rough estimate for the J_2 term of the most massive body. This part of the problem is not considered in this study.

The attraction by other celestial bodies have already been studied.[4] The main perturbing bodies are Gamma and Beta. The Sun and Mars then have an influence a thousand times smaller, and other planets and the asteroids Vesta, Pallas and Ceres have an influence more than 10000 times smaller. These relative influences increase with the distance of the spacecraft from the asteroids, but in this study the solution orbits stay well inside the sphere of influence of the asteroid system†.

The perturbations due to aerodynamic forces, electromagnetic forces, relativistic effects, albedo, spacecraft infra-red radiation, are all neglected. This choice is motivated by the literature about

*`http://nssdc.gsfc.nasa.gov/planetary/factsheet/earthfact.html`

†The sphere of influence has a radius of about 35 km, obtained with the following equation, assuming that all three masses are concentrated at the centre of the system: $r_{SOI} = a * \left(\frac{M_{asteroids}}{M_{Sun}}\right)^{2/5}$, with $a = 1.99\,\mathrm{ua}$, $M_{asteroids} = 9.5 \times 10^{12}\,\mathrm{kg}$ and $M_{Sun} = 1.9891 \times 10^{30}\,\mathrm{kg}$

previous studies for the ASTER mission to the 2001 SN263 asteroid,[2,7,13] but also about other past, future or current missions to primitive bodies[14,15] and general studies about astrodynamics and the environment around primitive bodies,[16–18] which are unanimous on the fact that these perturbations have a negligible effect compared to the uncertainty in the main forces considered in our model, and the other simplifications made in this study.

METHODOLOGY

The tool developed for this study initializes by pre-computing the ephemeris tables for Alpha, Beta and Gamma and setting up the population of spacecraft initial states to be propagated, then proceed to successive iterations of new generations of solutions. At each iteration, the tool propagates the trajectories for all initial states until the stopping condition is met and evaluate them against the objective functions of the scenario considered. The optimization algorithm then generates the next population to be evaluated, until the problem converged.

Multiple asteroid initial conditions

Although the exact orbit of all the asteroids are considered as known, the position of Beta and Gamma on their orbits are considered as unknown or uncertain for some of the mission scenarios in which the objective is to find optimum orbits regardless of these positions. The tool is able to consider multiple initial true anomalies for Beta and Gamma. At the moment of the evaluation of the objective function, a single value is returned, which can be the maximum (used for worst case scenarios), minimum (used to find best initial conditions) or average (to find results good in most cases).

Orbit propagation

The orbit propagator has been implemented mostly using tools available in the *Tudat* astrodynamics library*. The effects of all forces in the system are calculated using the models described here above. The position of Alpha, Beta and Gamma at a given time are interpolated from the pre-computed ephemeris tables, and the position of the Sun is fixed. The orbits of the primaries are independent of the initial conditions of the spacecraft, and hence are computed as a preliminary step. The trajectories of Beta and Gamma are propagated considering only the influence of the central body Alpha, until a maximum integration time sufficient for all spacecraft trajectory propagations to come. The trajectories are stored as tabulated ephemeris.

The integration itself is also taken care of by Tudat using a *Runge-Kutta 4 fixed step size integrator*, chosen mostly because it is the simplest reasonable choice: the Euler integrator is basically a first order Taylor approximation and is generally known not to yield reliable results in astrodynamics, and the Runge-Kutta variable step size integrators are of a higher complexity. The integration part is of lesser importance than the optimization process for this study and the Runge-Kutta 4 with fixed step performed well and is often used in other similar applications. Changing to a Runge-Kutta variable step size integrator might bring some improvements in terms of performances with regards to precision, but mostly in the case that more complex force models are considered to represent the system.

The integration step size has been chosen by propagating the initial state of a chosen actual solution until it crosses the return section for the 10th time, and studying its convergence. A time

*`https://github.com/tudat`

step of 600 s is a good compromise. It keeps the error below 1 m for the distance (smaller than the 20 m threshold used to consider orbits as closed) and 2×10^{-4} m s^{-1} for the delta-V, for a 4-day integration time, while keeping the computation time below 1 s, which is important as each optimization problem requires running millions of orbit propagations.

Return map and integration stopping condition

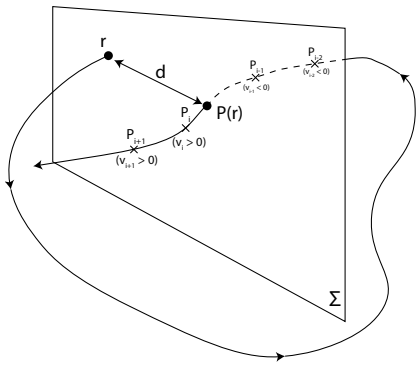

Figure 2: Principle of the return map: the Poincaré map P linked to the Poincaré section Σ projects point r onto point $P(r)$. Stopping condition of the integration: crossing is detected for the integration point P_i.

The use of a *return map* (or *Poincaré map*) is central for the software application. It serves as stopping condition for the orbit propagator, and it is used in the evaluation of the quality of closing of the orbit (*i.e.* its ability to come back to the initial state). The conceptual advantage of the *method of Poincaré* is to reduce the study of periodic orbits to the study of equilibrium points, as represented in Figure 2.

The choice of the position of the return section is classically dictated by symmetries in the system studied. In the case of the 2001 SN263 asteroid system, no symmetry can be found in the gravitational field. However, the fact that the solar radiation pressure is only directed towards $-x$ makes us expect a symmetry of the orbit with regards to any plane containing the x axis. The plane $(O, x, z)_{x>0}$ (or $y = 0|_{x>0}$) is chosen as return section.

The computation of the return map is integrated to the orbit propagation process. After every integration step, a test is done to detect if the spacecraft just crossed the return section. The last state undergoes a reference frame transformation between the inertial reference frame and the return section reference frame (named $(0, u, v, w)$ hereafter), in which the crossing condition is written $v = 0$. So the spacecraft just crossed the section at the i-th integration point if equation 3 is satisfied, where the crossing direction $C = +1$ goes from $v < 0$ to $v > 0$, and $C = -1$ from $v > 0$ to $v < 0$.

$$C * v_i > 0 \text{ AND } C * v_{i-1} < 0 \text{ AND } i \neq 0 \tag{3}$$

The integration is stopped when a certain number of section crossings is reached: 1 for a single loop of the spacecraft, more for multiple loops in the system. This stopping condition is to be

specified in the optimization problem. Once the orbit propagation is done, the exact position of the return points on the section is obtained by interpolation.

Objective functions

The propagation of the orbits returns the integrated state history, the return map, as well as a *result flag* which tells if the integration went well or was interrupted because of a crash with a body, achieving escape velocity, reaching the maximum integration time, or insufficient and excessive initial velocity. In these cases, any objective function is given a *penalty value*. Otherwise, from these primary results, the tool computes the so-called *secondary results*: closing distance, closing delta-V and fraction of the orbit spent in the observation zones of the three bodies. These secondary results are then used to compute the values for the objective functions, which are scalar values to be minimized. Several objective functions were implemented for the optimization and can be picked and combined to optimize various mission scenarios.

Closing distance $f_{\Delta dist}$. This function aims at characterising how well the spacecraft comes back to its initial position after a given number of crossing of the section of initial positions. It computes the Euclidean distance between the first and the last position vectors in the Poincaré map (Eq. 4).

Closing delta-V $f_{\Delta V}$. This function, similarly to the previous one, aims at determining how well the spacecraft comes back to its initial state, but this time looking at the delta-V between the initial and final velocity. This function is defined as the Euclidean distance between the first and the last velocity vectors in the Poincaré map (Eq. 5).

Combined closing function $f_{closing}$. This function combines in a single function both the closing distance and the closing delta-V. The value of the closing delta-V is only interesting if the orbit can be considered as closed. For states with a closing distance larger than a threshold distance considered as a "closed orbit", the function returns the (normalised) closing distance; for states with a closing distance smaller than the threshold, it is the normalised closing delta-V that is returned (Eq. 6). The threshold and normalisation values $\epsilon = 10\,\mathrm{m}$, $d_{ref} = 1\,\mathrm{m}$ and $V_{ref} = 1\,\mathrm{m\,s^{-1}}$ are chosen to make sure that, in general, $\frac{f_{\Delta V}}{V_{ref}} < \frac{\epsilon}{d_{ref}}$, or, for d_{ref} arbitrarily fixed at 1, $\frac{f_{\Delta V}}{V_{ref}} < \epsilon$. This "guides" the optimization by first minimizing the closing distance, then the closing delta-V. The values returned for an orbit considered as non-closed should always be larger than the values of the closing delta-V returned if the orbit is closed.

Body Observation function f_{obs}. This objective function determines how good a trajectory is at observing given bodies. The objective function will consider the fraction of the orbital time spent in this observation zone, defined by a minimum and a maximum observation distances. For each integration point of the trajectory, if the current position is in the observation zone, the time passed since the previous state is added (Eq. 7). The objective function f_{obs} (Eq. 9) combines the observation times of several bodies if desired: a score of 1 indicates poor observations conditions (at least one of the bodies is never at good observation distance), while a score of 0 indicates that the trajectory allows a good observation of all bodies considered 100 % of the time.

$$f_{\Delta dist} = \|X_{end} - X_{init}\| \tag{4}$$

$$f_{\Delta V} = \|V_{end} - V_{init}\| \tag{5}$$

$$f_{\text{closing}} = \begin{cases} \frac{f_{\Delta dist}}{d_{ref}} & \text{if } f_{\Delta dist} > \epsilon \\ \frac{f_{\Delta V}}{V_{ref}} & \text{otherwise} \end{cases} \tag{6}$$

$$T_B = \sum_{i=1}^{n-1} \begin{cases} t_i - t_{i-1} & \text{if } d_{min} < d_B < d_{max} \\ 0 & \text{otherwise} \end{cases} \tag{7}$$

$$F_B = \frac{T_B}{t_n - t_0} \tag{8}$$

$$f_{\text{obs}} = 1 - \prod_B F_B \tag{9}$$

Optimization

The implementation of the optimization problem was done using the PaGMO (Parallel Global Multiobjective Optimiser) library*, a software tool for high-dimensional global optimization.[19] It includes a variety of optimization algorithms, supports numerous types of optimization problems and has been designed to provide an easy implementation on parallel threads.

Optimization problem. Working with PaGMO starts with the definition of a problem. Every individual of the population during the optimization problem is represented by an instance of this problem. The problem is initialized with the upper and lower boundary vectors (delimiting the search space), the number of constraints of the problem fixed to 0, and the dimension of the fitness vector (1 or 2 in this study). The objective functions implementation reads the decision vector of the individual (five-dimensional initial conditions of the spacecraft) and runs the orbit propagation for each of the problem parameters contained in the problem list. It then computes and returns a fitness vector as specified in the input (dimension and functions to compute).

Setting up of the archipelago. PaGMO represents the optimization problem as an *archipelago*, which contains the set of islands collaborating in the optimization process. This allows to increase the total size of the population while allowing the parallelisation of the optimization process. Each *island* is populated by individuals and is given the same optimization method. The *topology* of the archipelago is the migration policy of individuals between the islands. In the absence of a specific reason to select another topology, the "fully connected" topology is a good default choice,[19] which means that individuals can migrate both ways between any two islands.

Self-adaptive Differential Evolution (jDE). This algorithm is used for all use cases that have a single objective function. It is an enhancement of the original Self-adaptive Differential Evolution algorithm (SaDE).[20] Its main idea[21] is the introduction of two adaptation methods. The first is a *strategy adaptation*, whose allow the algorithm to learn which are the mutation strategies that produce the most successful mutants and change their probability of being used accordingly. The second is a *parameter adaptation* which removes the necessity to choose F, a mutation scaling factor, and CR, the crossover constant, which both require to be adapted to the problem's properties and complexity, and let the algorithm choose them using probability laws and a learning strategy.

*https://esa.github.io/pagmo/

Multiobjective Evolutionary Algorithm Based on Decomposition. This method (MOEA/D) is *multiobjective* because it looks for optima according to several objective functions (the solutions have a fitness vector instead of a fitness value). *Decomposition* consists of breaking the problem down into several subproblems to optimize. Unlike most multiobjective optimization evolutionary algorithms which treat the multiobjective optimization problem as a whole and rely on domination between solutions, MOEA/D decomposes the problem into scalar optimization subproblems that are optimized simultaneously. Each sub-problem is optimized by only using information from its neighbouring sub-problems. This method typically has a lower computation time thanks to a lower computational complexity and yields very uniform Pareto fronts thanks to a very natural decomposition method.[22]

Mission scenarios

The tool is run on three different cases, each one corresponding to a phase of the mission or a scenario considered for the exploration of the system. These scenarios are translated into parameters, constraints and objective functions and given as inputs to the tool.

General parameters for the propagator and optimizer. In total, the tool requires more than 60 input parameters. Among these, some are fixed and common to all use cases: orbital characteristics (refer to Table 1) except the true anomalies of Beta and Gamma, physical properties of the spacecraft (mass of 150 kg, cross section area of 20 m^2, radiation pressure coefficient of 1.21), orbit propagation parameters (16 000 000 s maximum integration time, 600 s time step, 10 000 s minimum integration time, 20 m closing tolerance) and optimization parameters (4 islands in the archipelago, 100 individuals on each island, 2000 generations maximum).

Case 1: Arrival parking orbit. Following its interplanetary travel, the ASTER probe will arrive at the 2001 SN263 system with little or no knowledge of the relative positions of the asteroids. The spacecraft should hence be put on an safe orbit from which the spacecraft can make the preliminary studies of the dynamics of the system. This orbit should have good closing properties to ensure repeatability and stability, have as little dependence on the initial position of the asteroids as possible, stay outside the system, at good distance from any body to avoid collision, and allow a first study from a distance of the dynamics of the system. This scenario translates into the optimization parameters presented in Table 2.

The first results obtained for these parameters had a very limited lifespan (1 to 4 days until crash with Alpha) that disqualified them from any practical use. This is due to the fact that solutions for this case are by nature very close to Alpha and have a very short orbital period, between 5 and 7 hours, and will have to repeat tens to hundreds of times to reach weeks. Imperfections in the closing of the orbit and deviations induced by the moving bodies cause the trajectory to deviate greatly. To circumvent this issue, the 10th return point is considered, instead of the 1st, so that the spacecraft completes several revolutions about Alpha. This guaranties that the trajectories will be propagated during at least 2 days. This produced much better results, which are presented here after.

Case 2: Orbits for sequential exploration scheme. As one of the schemes considered for exploring the asteroids system, the spacecraft passes through successive orbits, each one of them being designed for an optimal observation of only one given body. For this case, it is reasonable to assume that at least the position of the body to observe is known, and is chosen arbitrarily, while the position of the other bodies is taken as an unknown parameter. Three orbit searches are necessary, one for each body of the system. These three optimization problems are named 2-Alpha, 2-Beta and

2-Gamma, respectively. These orbits should have good observation conditions, and good closing conditions for the repeatability of the orbit. This scenario translates into the optimization parameters presented in Table 3.

Case 3: Trajectories for parallel exploration scheme. In this scenario, the spacecraft is on a single trajectory that should allows the observation of each body for at least a portion of the trajectory. For this phase, it is considered that the position of all bodies is known precisely, and that the spacecraft can be inserted in the observation orbit whenever wanted. We are hence looking for the best case solution regarding the initial positions of Beta and Gamma. The lifespan of these orbits, and even whether it is possible to repeat and maintain it for several revolutions, is to be defined by this analysis. It is indeed expected that after one revolution of the spacecraft, as Beta and Gamma will have different positions, repeating the same orbit with the same observation conditions will not be possible. These orbits should have good observation conditions of all three bodies, good closing distance conditions for the orbit to have the spacecraft coming back to its initial condition. As a manoeuvre using thrust is probably going to occur at the beginning and the end of the orbit, the continuity of the velocity at the closing point is not necessary. This scenario translates into the optimization parameters presented in Table 4.

Table 2: Optimisation parameters for test case 1
[1]: Distance from the centre of the body considered. Subtract body radius to get the distance from the body surface (Alpha: 1300 m, Beta: 420 m, Gamma: 342 m).
[2]: Distance from the centre of Alpha.

Test case		1
Search space	x [m]	$[0, 50000]$
	z [m]	$[-50000, 50000]$
	V_x [m s^{-1}]	$[-0.8, 0.8]$
	V_y[m s^{-1}]	$[-0.8, 0.8]$
	V_z[m s^{-1}]	$[-0.8, 0.8]$
Beta initial true anomalies [rad]		$\{0, \frac{\pi}{2}, \pi, \frac{3\pi}{2}\}$
Gamma initial true anomalies [rad]		$\{0, \frac{\pi}{2}, \pi, \frac{3\pi}{2}\}$
Objective functions	f_0	f_{closing} (average)
Crash distances[1]	Alpha [m]	6300
	Beta [m]	5420
	Gamma [m]	5342
Escape distance[2] [m]		100000

RESULTS AND ANALYSIS

In this section, solutions are identified by their initial conditions given as a state vector $[x, z, V_x V_y V_z]$. In plots of trajectories, Alpha is represented as a purple sphere, Beta as the blue sphere on the outer circular orbit, and Gamma as the red sphere on the inner circular orbit. The initial position of the spacecraft is the yellow diamond, and its trajectory a black line.

Parking orbits

For the case 1, the optimization yielded solutions that can be clearly classified into two families with very similar initial conditions and properties, but revolving in the other direction. Type

Table 3: Optimisation parameters for test case 2
[1]: Distance from the centre of the body considered. Subtract body radius to get the distance from the body surface (Alpha: 1300 m, Beta: 420 m, Gamma: 342 m).
[2]: Distance from the centre of Alpha.

Test case		2-Alpha	2-Beta	2-Gamma
Search space	x [m]	$[0, 15000]$	$[16382, 30000]$	$[0, 20000]$
	z [m]	$[-15000, 15000]$	$[-15000, 15000]$	$[-15000, 15000]$
	V_x [m s^{-1}]	$[-0.8, 0.8]$	$[-0.33, 0.33]$	$[-0.8, 0.8]$
	V_y[m s^{-1}]	$[-0.8, 0.8]$	$[0.7, 0.33]$	$[-0.8, 0.8]$
	V_z[m s^{-1}]	$[-0.8, 0.8]$	$[-0.33, 0.33]$	$[-0.8, 0.8]$
Beta initial true anomalies [rad]		$\{0, \frac{\pi}{2}, \pi, \frac{3\pi}{2}\}$	0	0
Gamma initial true anomalies [rad]		$\{0, \frac{\pi}{2}, \pi, \frac{3\pi}{2}\}$	$\{0, \frac{\pi}{2}, \pi, \frac{3\pi}{2}\}$	0
Objective functions	f_0	f_{closing} (average)	f_{closing} (average)	f_{closing} (average)
	f_1	$f_{\text{obs}}(\alpha)$ (average)	$f_{\text{obs}}(\beta)$ (average)	$f_{\text{obs}}(\gamma)$ (average)
Crash distances[1]	Alpha [m]	1500	1500	1500
	Beta [m]	620	620	620
	Gamma [m]	542	542	342
Escape distance[2] [m]		50000	50000	50000
Observation zone[1]	Alpha [m]	$[1800, 11300]$	-	-
	Beta [m]	-	$[920, 10420]$	-
	Gamma [m]	-	-	$[352, 1342]$

Table 4: Optimisation parameters for test case 3
[1]: Distance from the centre of the body considered. Subtract body radius to get the distance from the body surface (Alpha: 1300 m, Beta: 420 m, Gamma: 342 m).
[2]: Distance from the centre of Alpha.

Test case		3
Search space	x [m]	$[0, 30000]$
	z [m]	$[-30000, 30000]$
	V_x [m s^{-1}]	$[-1, 1]$
	V_y[m s^{-1}]	$[-1, 1]$
	V_z[m s^{-1}]	$[-1, 1]$
Beta initial true anomalies [rad]		$\{0, \frac{\pi}{2}, \pi, \frac{3\pi}{2}\}$
Gamma initial true anomalies [rad]		$\{0, \frac{\pi}{2}, \pi, \frac{3\pi}{2}\}$
Objective functions	f_0	f_{closing} (average)
	f_1	$f_{\text{obs}}(\alpha, \beta, \gamma)$ (minimum)
Crash distances[1]	Alpha [m]	1500
	Beta [m]	620
	Gamma [m]	542
Escape distance[2] [m]		50000
Observation zone[1]	Alpha [m]	$[1800, 6300]$
	Beta [m]	$[920, 5420]$
	Gamma [m]	$[842, 5342]$

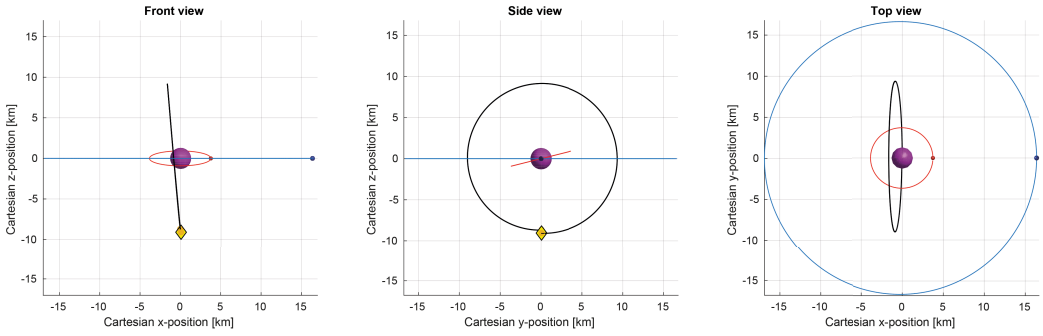

(a) Type A solution

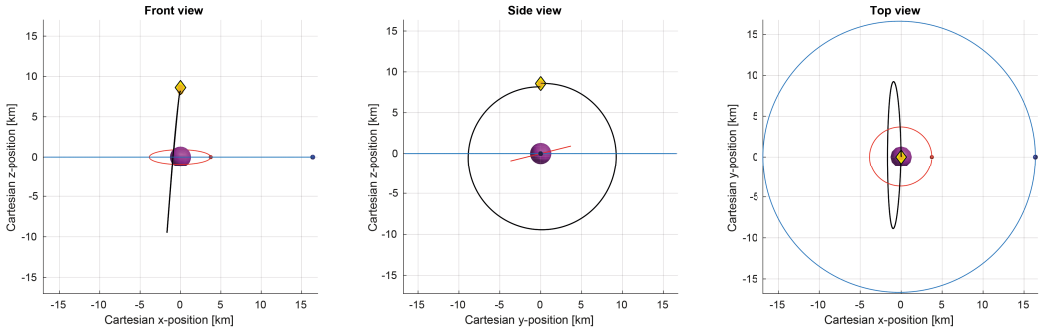

(b) Type B solution

Figure 3: Case 1: trajectory of solutions from families A and B

A are retrograde orbits starting directly below Alpha ($0\,\mathrm{m} < x < 7\,\mathrm{m}$ and $-9074\,\mathrm{m} < z < -9023\,\mathrm{m}$) with an initial velocity vector mostly pointing towards $+y$ ($0\,\mathrm{m\,s^{-1}} < V_x < 0.001\,\mathrm{m\,s^{-1}}$, $0.259\,\mathrm{m\,s^{-1}} < V_y < 0.261\,\mathrm{m\,s^{-1}}$, $V_z \approx 0.010\,\mathrm{m\,s^{-1}}$). Type B are prograde orbits starting directly above Alpha ($0\,\mathrm{m} < x < 8\,\mathrm{m}$ and $8572\,\mathrm{m} < z < 8576\,\mathrm{m}$) with an initial velocity vector mostly pointing towards $+y$ as well ($V_x \approx 0.005\,\mathrm{m\,s^{-1}}$, $0.271\,\mathrm{m\,s^{-1}} < V_y < 0.272\,\mathrm{m\,s^{-1}}$, $V_z \approx 0.011\,\mathrm{m\,s^{-1}}$).

The solution of type A chosen for analysis has the following initial conditions: $[2.42\,\mathrm{m}, -9071.2\,\mathrm{m}, -0.0003\,\mathrm{m\,s^{-1}}, 0.2592\,\mathrm{m\,s^{-1}}, -0.0106\,\mathrm{m\,s^{-1}}]$. The solution of type B chosen for analysis has the following initial conditions: $[1.184\,\mathrm{m}, 8574.47\,\mathrm{m}, -0.0049\,\mathrm{m\,s^{-1}}, 0.272\,\mathrm{m\,s^{-1}}, 0.0116\,\mathrm{m\,s^{-1}}]$. These two solutions have the best fitness of their families (respectively 343.8 and 318). Figure 3 shows the two trajectories in the inertial reference frame, for the sets of initial conditions for Beta and Gamma $\theta_{\beta 0} = 0$ and $\theta_{\gamma 0} = 0$. These trajectories are eccentric polar orbits about Alpha with a radius of about 18 km in the (O, x, y) plane. The effect of the solar radiation pressure is clearly visible as the orbit is pushed away from the direction of the Sun, and the centre of Alpha is outside the orbital plane. They have a period of 2 d 19 h 42 min and 2 d 18 h 24 min respectively.

The initial position for the bodies Beta and Gamma has a major impact on the properties of the orbit. The closing distance of the orbits varies between 18 m and 796 m. Overall, the orbits have very poor closing, and hence poor orbit repeatability: both the average 300 m and worst case (700 m) values are well above the 20 m threshold to consider the orbit as a closed one. The closing

delta-V has a more reasonable value and is anyway secondary, as the high closing distance is the main reason why the orbit will not close and repeat itself. Despite this low repeatibility, a long-term study of the orbit shows that the orbit, initially mostly circular, undergoes a slow precession and increase of its eccentricity, but does not come closer than 3.5 km from the surface of any body over a three-month integration period, and hence is rather safe.

Nevertheless, the location of the orbits, inside the system between the orbits of Beta and Gamma, make them unfit for a use as first orbit upon arrival in the system. In the absence of good knowledge on the position of Beta and Gamma on their orbits, and considering the doubt there is on the accuracy on the orbital parameters of the asteroid moons, setting up an insertion manoeuvre to this orbit will be risky as Beta might be in the way.

Close up observation of Alpha

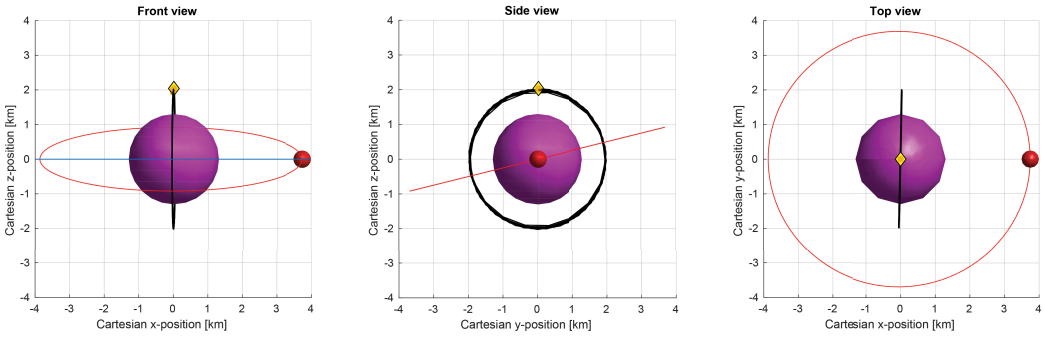

Figure 4: Case 2-Alpha: trajectory of a solution from family B (Beta is left out of the figure)

For the case 2-Alpha, the optimization yielded solutions that can be classified into two families of orbits that have very similar properties, Type B being the retrograde version of type A. This study focuses on a type B solution, as solution of type B slightly dominate the solutions of type A, and they are so similar that the analysis and conclusions made here below also apply to the type A solutions. Type B are prograde orbits starting above Alpha ($0\,\mathrm{m} < x < 903\,\mathrm{m}$ and $1548\,\mathrm{m} < z < 2512\,\mathrm{m}$) with an initial velocity vector mostly pointing towards $+y$ ($-0.024\,\mathrm{m\,s^{-1}} < V_x < 0.055\,\mathrm{m\,s^{-1}}$, $0.433\,\mathrm{m\,s^{-1}} < V_y < 0.659\,\mathrm{m\,s^{-1}}$, $-0.014\,\mathrm{m\,s^{-1}} < V_z < 0.029\,\mathrm{m\,s^{-1}}$).

Despite their similarities, the solutions have a wide range of scores in the fitness functions and form a well-distributed Pareto front. If the value for the closing function ($f_{closing}$) stays between 15.43 and 30, which is in the order of the 20 m threshold for closed orbits, the spacecraft spends between 100 % and only 19 % of its orbit in the observation zone. The orbital period of the solutions varies between 2 h 15 min and 6 h 45 min 45 s. Their lifespan (always ending with a crash with Alpha, varies greatly between 2 days, which is clearly insufficient, to over 88 days, which is more than enough for a close-up orbit.

The solution of type B, shown in Figure 4, chosen for analysis has the following initial conditions: $[0\,\mathrm{m}, 2029.81\,\mathrm{m}, 0.010\,738\,\mathrm{m\,s^{-1}}, 0.544\,606\,\mathrm{m\,s^{-1}}, 0.000\,256\,\mathrm{m\,s^{-1}}]$. It is a low polar circular orbit in the (O, y, z) plane around Alpha, with a radius of about 2 km. It scores a 27 m average closing distance and a perfect 100 % capability for observing Alpha by staying close to the lower bound of the observation zone.

The invariance with regard to the 16 combinations of initial positions for Beta and Gamma is well contained: the closing distance vary between 4.17 m and 61.62 m, and the closing velocity between 0.004 m s^{-1} and 0.024 m s^{-1}. Although this variance cannot be neglected, the orbit proved robust against them, as the orbital period varies only between 6 h 15 min 52 s and 6 h 19 min 46 s, the observation capability of Beta is not impacted at all, and the orbit remains stable and has a good long-term stability, above 2 months in the worst case.

Close up observation of Beta

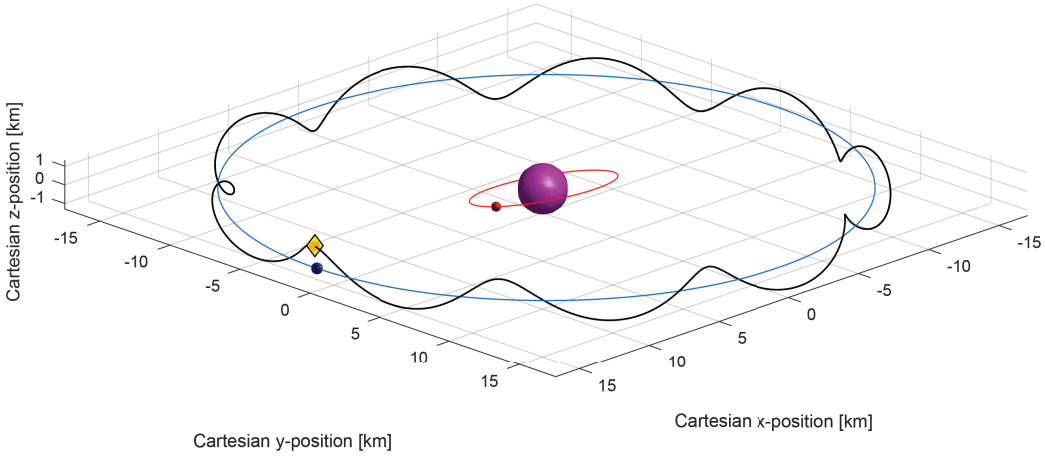

Figure 5: Case 2-Beta: trajectory of a solution from family A1

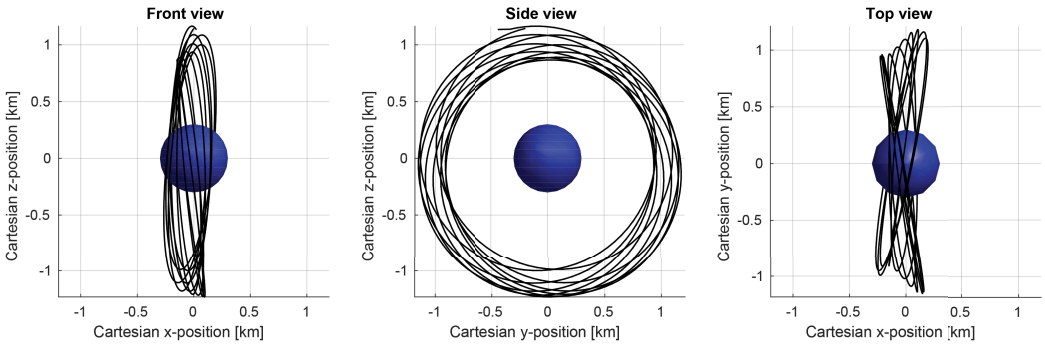

Figure 6: Case 2-Beta: trajectory in the Beta-centred reference frame of a solution from family A1

Previous cases converged to well-distributed Pareto fronts. The case 2-Beta, however, converged here to the very limited number of 35 optima. The problem hqs been run 10 times to ensure repeatibility. All orbits are similar, that can be distinguished by their direction of rotation about Beta (type A or B). Type A are orbits starting on top of Beta ($16\,382\,\mathrm{m} < x < 16\,397\,\mathrm{m}$ and $1097\,\mathrm{m} < z < 2098\,\mathrm{m}$) with an initial velocity vector mostly pointing towards $+y$ ($-0.304\,\mathrm{m\,s^{-1}} < V_x < -0.0035\,\mathrm{m\,s^{-1}}$, $0.0769\,\mathrm{m\,s^{-1}} < V_y < 0.1396\,\mathrm{m\,s^{-1}}$, $-0.031\,\mathrm{m\,s^{-1}} < V_z < 0.0716\,\mathrm{m\,s^{-1}}$). Type B are orbits starting below Beta ($16\,382\,\mathrm{m} < x < 16\,452\,\mathrm{m}$ and $-2088\,\mathrm{m} < z < -916\,\mathrm{m}$) with an

initial velocity vector mostly pointing towards $+y$ as well ($-0.0147\,\mathrm{m\,s^{-1}} < V_x < -0.0096\,\mathrm{m\,s^{-1}}$, $0.0700\,\mathrm{m\,s^{-1}} < V_y < 0.1394\,\mathrm{m\,s^{-1}}$, $-0.0459\,\mathrm{m\,s^{-1}} < V_z < 0.0399\,\mathrm{m\,s^{-1}}$).

These optima roughly follow an inverse law in the $(f_{\text{closing}}, f_{\text{obs}}(\beta))$ plane, which shows that the two objectives are conflicting. A trade-off has to be done between the solutions (marked with the suffix 2) favouring a good closing of the orbit at the cost of a bad capacity of observation of Beta (typically, $f_{\text{obs}}(\beta) > 0.15$), and the ones, marked with suffix 3, with very good ability to observe Beta ($f_{\text{obs}}(\beta) \approx 0$), but a poor quality of closing (typically $f_{\text{closing}} > 20\,\mathrm{m}$). Solutions A1 and B1 are the ones considered to have the best compromises ($f_{\text{closing}} < 25\,\mathrm{m}$, $f_{\text{obs}}(\beta) < 0.1$). For the same reason as the previous cases, only a solution of type A1 is studied here, but the conclusions are still valid for type B1.

The solution of type A1 chosen for analysis has the following initial conditions: $[16\,382.4\,\mathrm{m}$, $1144.54\,\mathrm{m}, -0.0231\,\mathrm{m\,s^{-1}}, 0.0876\,\mathrm{m\,s^{-1}}, -0.0251\,\mathrm{m\,s^{-1}}]$. Plotted in the inertial reference frame (Figure 5), this trajectory has the shape of a spring winded around the trajectory of Beta. In a Beta-centred reference frame (Figure 6), it appears as a polar orbit in the (x, z) plane, with a radius of about 1 km, is slowly precessing over time. During one orbital period about Alpha, the spacecraft achieves exactly 10 revolutions about Beta for an orbital period of about 15 h.

This solution stays more than 90 % of the time in the observation zone of Beta. The variation of the orbit depending on the initial position of Gamma is limited: closing distance between 13.10 m and 26.46 m, closing velocity between 0.035 m s^{-1} and 0.054 m s^{-1}. Its orbital period (about Alpha) is between 6 d 7 h 2 min 44 s and 6 d 7 h 31 min 21 s. This imperfection in the closing makes the orbit slowly undergoes a precession and increase of its eccentricity, until it crashes with Beta after 17 d 21 h 20 min in the worst scenario, which allows it to complete 2 revolutions about Alpha. If a longer lifespan is necessary, one could consider using an impulsive delta-V after every period to correct for the imperfection in the delta-V. Considering the worst case, a 0.054 m s^{-1} impulse every 6.3 days represents 0.26 m s^{-1} of delta-V over a month, so 5 % of the manoeuvring fuel on ASTER.

Absence of suitable orbits for close up observation of Gamma

The scenario 2-Gamma is a special case. Initially, it had the same problem parameters as the cases 2-Alpha and 2-Beta. No satisfying solution could be found, as all solutions found were low orbits about Alpha with really poor observation ability of Gamma, so the problem parameters have been changed. Although a margin of 200 m added to the body radius to obtain the crash distance for all cases, this margin has been removed around Gamma for the case 2-Gamma. The observation zone around other bodies is between 300 m and 10 km, but between 10 m and 1 km for Gamma. Another exception is that a single arbitrary initial true anomaly of Beta is considered. With these changes, the initial scenario hence moved to the one of a very close approach of Gamma for detailed study of the surface.

The lack of results for the initial scenario is not surprising. First of all, the sphere of influence of Gamma with regards to Alpha is too small, 618 m of radius, smaller than the collision distance with Gamma of 842 m, to imagine finding a trajectory around Gamma within the observation zone. Secondly, a previous study[2] showed that there was indeed no stability region about Gamma.

Close approach to observe Gamma

For the case 2-Gamma, the tool produces a lot of distinct solutions, which require 12 families to classify them. Three families of orbits have been selected for analysis: B, T and Q. The other

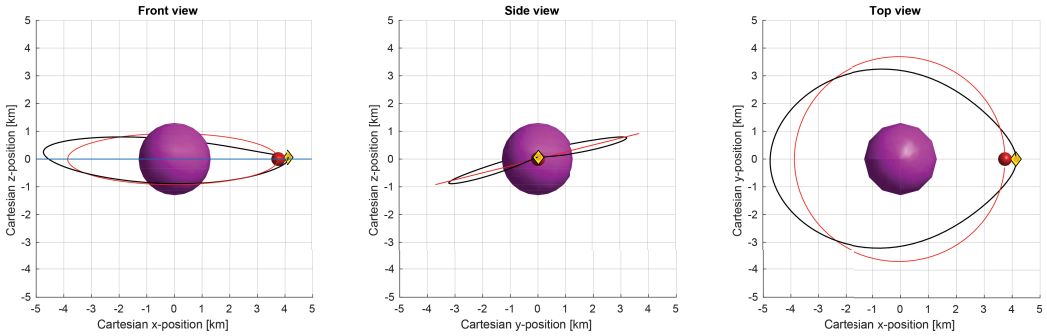

(a) Type B

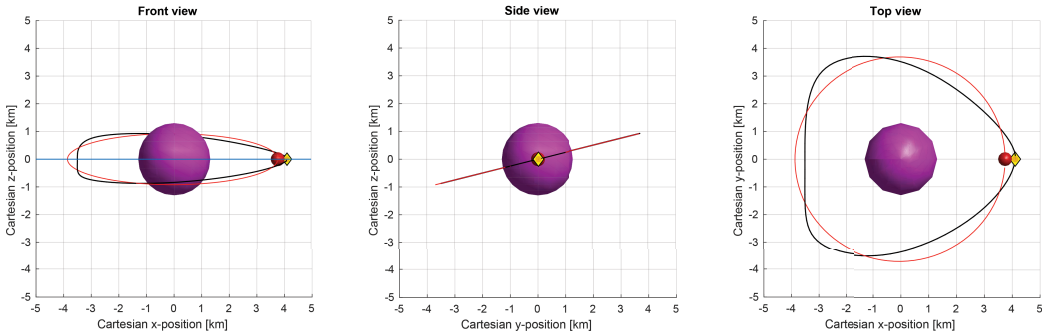

(b) Type T

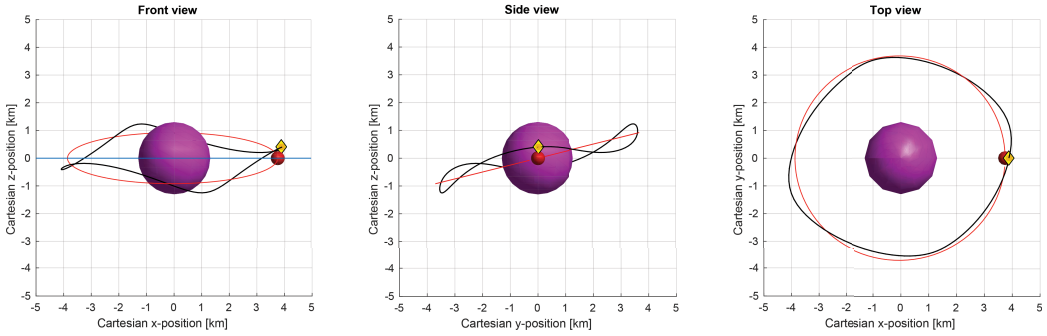

(c) Type Q

Figure 7: Case 2-Gamma: trajectories in the inertial reference frame (Beta is left outside the figure)

families have been discarded because of some properties that made them unusable: orbit staying less than 50 % of the time in the observation zone, lifespan too short with regards to its orbital period, or closing delta-V too high with no added advantage compared with the selected options.

The chosen solution of type B, represented in Figure 7a, has the following initial conditions: $[4144.0\,\mathrm{m}, 59.3\,\mathrm{m}, -0.0081\,\mathrm{m\,s^{-1}}, 0.2617\,\mathrm{m\,s^{-1}}, 0.023\,64\,\mathrm{m\,s^{-1}}]$. It has been selected for having the biggest lifespan, and has an orbital period of 16 h 35 min 26 s. The chosen solution of type T, represented in Figure 7b, has the following initial conditions: $[4117.7\,\mathrm{m}, -3.8\,\mathrm{m}, 0.0073\,\mathrm{m\,s^{-1}},$

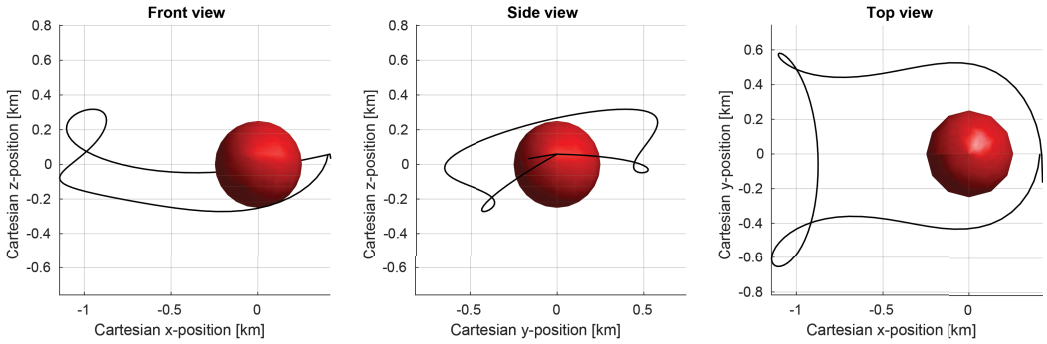

(a) Type B

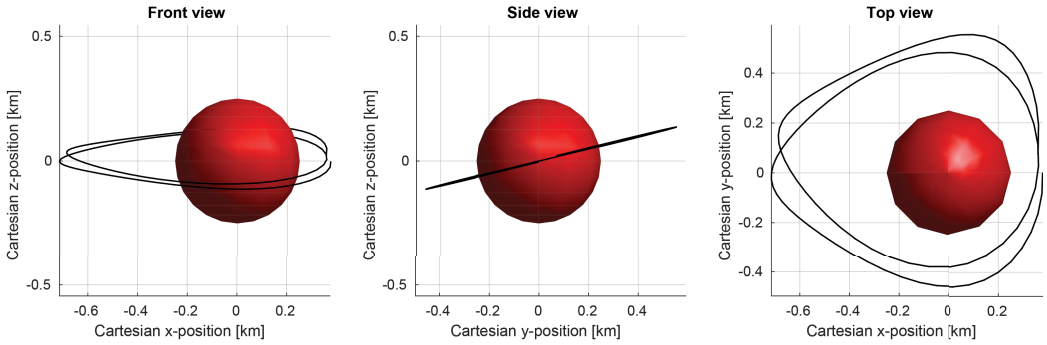

(b) Type T

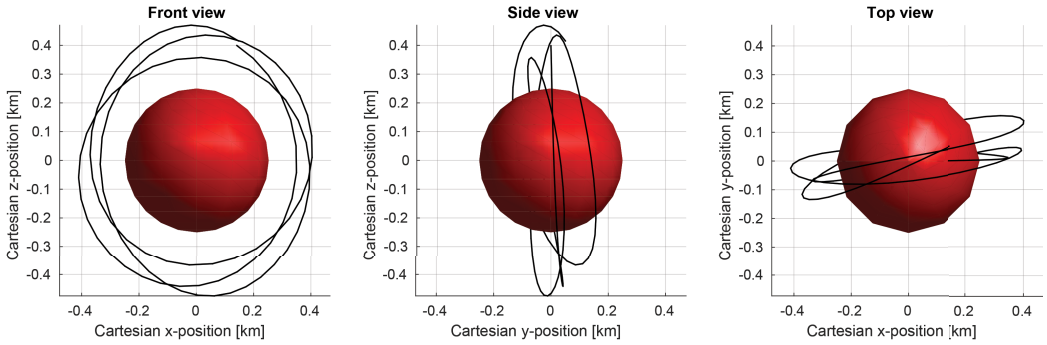

(c) Type Q

Figure 8: Case 2-Gamma: trajectories in the Gamma-centred reference frame

$0.2527\,\mathrm{m\,s^{-1}}, 0.0632\,\mathrm{m\,s^{-1}}]$. It has been selected for having a slightly better score at the closing function. It has an orbital period of 16 h 27 min 30 s. The chosen solution of type T, represented in Figure 7c, has the following initial conditions: $[3880.6\,\mathrm{m}, 400.8\,\mathrm{m}, 0.1006\,\mathrm{m\,s^{-1}}, 0.3975\,\mathrm{m\,s^{-1}}, 0.0342\,\mathrm{m\,s^{-1}}]$. It has been selected for having a slightly better score at the closing function. It has an orbital period of 16 h 30 min 47 s.

These three selected families are either planar (B and T) or oscillating (Q) with an orbital plane in the orbital plane of Gamma. They all start about at the same initial position outside the orbit of Gamma ($x \approx 4\,\mathrm{km}$), and are revolving about it. Looking from a Gamma-centred reference frame, as seen in Figure 8, the type B has a very complex 3-dimensional shape, the type T is perfectly planar with a drop shape, and the orbit Q is a highly perturbed polar circular orbit. The orbital periods of all orbits are very close to the 16 h 32 min 10 s orbital period of Gamma, which makes sense as the spacecraft remains close to Gamma.

All three orbits are considered as closed (respectively 18.56 m, 19.99 m and 11.91 m closing distance and 0.0773 m s^{-1}, 0.0033 m s^{-1} and 0.0389 m s^{-1} closing delta-V). Despite having good closing properties, after an orbital period, Beta has moved about 39° on its orbit, so these orbits will deviate greatly from their original trajectory. Only the type B solution has a reasonable lifespan before colliding with Gamma, while T and Q are ephemeral (respectively 7 d 12 h 40 min, 16 h 40 min and 1 d 5 h 20 min). All solutions offer very good observation capabilities (respectively 100 %, 100 % and 95 %) inside the observation zone.

All solutions come extremely close to the surface of Gamma and are hence particularly risky to use. Furthermore, these results should be considered as valid for a single revolution about Alpha and for a single initial state of the system, chosen arbitrarily in this study. Yet, as all solutions orbits have the very interesting characteristics of having the same orbital period as Gamma, the change in the state of the system, after every revolution, is simply reduced to the initial position of Beta. Hence, designing an orbit with both a repeating shape and a lifespan longer than a single revolution is feasible by propagating the orbit by segments of one orbital period. For each segment, the initial position of Beta is set to its final position in the previous segment. The discontinuity in the velocity between the segments will be compensated by impulsive thrusts.

Absence of suitable orbits for parallel observation of all three bodies

For the case 3, no suitable solution could be found. Every run of the optimization produces the same results: polar orbits very low around Alpha, with a very poor or nonexistent ability to observe all three bodies ($f_{\mathrm{obs}}(\alpha, \beta, \gamma) = 0.98$ in the best case), as this kind of orbit never gets close to Beta, and only occasionally to Gamma.

Several tentatives were done to modify the parameters of the optimization problem to determine whether the lack of solutions was inherent to the geometry of the problem or due to a wrong translation of the scenario into an optimization problem. First of all, the same optimization problem was run multiple times to see if there was an issue with the exploration capabilities of the optimization algorithm. Modifying the boundaries of the observation zone or limit the observation function to the bodies Alpha and Beta, instead of all three, modified the value of the fitness function, but did not produce different kind of orbits. Other aggregation methods for managing the multiple initial positions of Beta and Gamma have been tried, by returning the average or maximum value instead of the minimum. But this worsens the results, which is logical given that returning the minimum is the less constraining aggregation method. It has been concluded that no closing orbit satisfying the case 3 can be found.

Predominance of terminator orbits

Most optima for all cases are polar or highly inclined orbits. These orbits, about Alpha or Beta, have their orbital plane relatively parallel to the (O, y, z) plane, perpendicular to the Sun direction $(+x)$. The fact that the optimization algorithm would favour terminator orbits was a result expected

from previous studies of trajectories of spacecraft around asteroids,[16] and is due to the solar radiation pressure. This force tends to push the spacecraft away in the $-x$ direction. A terminator orbit is an efficient and robust way to counteract this perturbation and allow the orbit to close in on itself. As the combined closing function is an objective function for all scenarios, it is normal that this kind of orbit plays an important role in this study. This indicates that the solar radiation pressure is a very important perturbation, at least as much as the minor bodies of the asteroid system.

Predominance of low orbits

The optimizer often favours orbits with a small semi-major axis. The orbits are either very close to the collision distance (case 1), or very close to the lower bound of the observation zone of the body considered (cases 2-Alpha, 2-Beta, and 2-Gamma). This might even be an issue when considering the whole lifespan of the orbits: any small change, perturbation or deviation over time is sufficient to have the spacecraft collide with a body or leave the observation zone. Despite this inconvenient, the optimizer never seem to find an advantage of having orbits further from the bodies.

This behaviour is actually understandable. Staying as close as possible to one of the body helps to improve the stability of the orbit by increasing the relative strength of the gravitational attraction of that body. This allows to reduce the perturbations coming from the other bodies, as well as the perturbations due to the solar radiation pressure, whose strength is constant in the system. On the contrary, for a distance from any body too big, the solar radiation pressure becomes too strong to be compensated by the gravitational attraction, and the solar radiation will blow the spacecraft away from the asteroid system. As an example, if the solar radiation pressure is turned off for the case 1, the tool produces an optima with a high apoapsis at about 70 km, with perfect closing properties, repeatability, indifferent of the initial position of Beta and Gamma. But, when taking the solar radiation pressure into account, this kind of orbit does not exist.

As a result, for any case, the choice on the collisions distances and/or the observation zone lower boundaries is of prime importance, because the optimum trajectories are very likely to come very close to these values.

CONCLUSION

As a general rule, terminator orbits with a small radius are the most suitable orbits within the asteroid system. They are the most adapted to counteract the very strong perturbations undergone in the system, primarily from the solar radiation pressure, secondly from the other bodies. Interesting low terminator orbits have been proven to exist around Alpha and Beta. Orbits complex shapes have been found about Gamma as well, but they are extremely low (a few tens of metres from its surface) and hence more risky.

This work cannot conclude on a satisfying parking orbit for the mission. No appropriate closed orbit has been found outside the system (*i.e.* past the orbit of Beta), because of the blow of the solar radiation that prevents the existence of orbits with a semi-major axis larger than a few kilometres.

For the exploration of the 2001 SN263 asteroid system, this study drive the choice towards a *sequential exploration scheme*, as no satisfying orbit for a parallel exploration scheme has been found. Terminator orbits about respectively Alpha and Beta allow to observe these bodies at a few kilometres for reasonable periods of time, at least several weeks or months, before the perturbations deviate the orbits sufficiently to have a danger of collision or escape the system.

The problem to optimize has typically the level of complexity that prevents the use of traditional optimization methods. The meta-heuristic approach to this problem proved to be very efficient, as it does not need an understanding of the equations ruling the motion of the spacecraft. This is taken care of by the numerical integrator, treated as a "black box" by the optimizer, which only considered its output.

Very good exploration capabilities allowed the optimizer to successfully find optima despite a very large search-space, and with no need to be "guided" towards preconceived solutions. It behaved in a very consistent way and confirmed produced coherent results. Proof of this is the predominance of terminator orbits, which was an expected result.

NOTATION

G	universal gravitational constant
m_i	mass of body i
r_i	distance from body i to the spacecraft
$\mathbf{e}_i$	unit vector from body i to the spacecraft
C_R	radiation pressure coefficient of the satellite
W	power density of the incoming radiation
A	effective cross-sectional area of the spacecraft
$m_{S/C}$	mass of the spacecraft
c	speed of light
T_B	time spent in the observation zone of a body B
F_B	fraction of time spent in the observation zone of body B
X	position of the spacecraft as a 3D-vector
V	velocity of the spacecraft as a 3D-vector
$init$	initial state
end	final state
d_{ref}	reference distance used to normalize the closing distance
V_{ref}	reference velocity used to normalized the closing delta-V
ϵ	tolerance on the closing distance to consider the orbit as closed
t_i	time of the state i
d_B	Euclidian distance from the centre of body B to the spacecraft
d_{min}	minimum observation distance
d_{max}	maximum observation distance
$\theta_{\beta 0}$	initial true anomaly of Beta
$\theta_{\gamma 0}$	initial true anomaly of Gamma

REFERENCES

[1] B. Sarli, O. Winter, P. Paglione, and E. Neto, "Strategies for exploring the triple system 2001sn263—target of the aster mission," *39th COSPAR scientific assembly, Mysore, India*, Vol. 1680, 2012.

[2] R. Araujo, O. Winter, A. Prado, and A. Sukhanov, "Stability regions around the components of the triple system 2001 SN263," *Monthly Notices of the Royal Astronomical Society*, Vol. 423, No. 4, 2012, pp. 3058–3073.

[3] A. G. V. d. Brum, A. Hetem Jr, C. Francisco, A. Fenili, F. Madeira, F. Cruz, and M. Assafin, "Preliminary development plan of the ALR, the laser rangefinder for the ASTER deep space mission to the 2001 SN263 asteroid," *J Aerosp Technol Manag JATM*, Vol. 3, 2011, pp. 331–338.

[4] A. F. Prado, "Mapping orbits around the asteroid 2001SN263," *Advances in Space Research*, Vol. 53, No. 5, 2014, pp. 877–889.

[5] P. Fin and R. Intini Marques, "PROGRESS ON THE DEVELOPMENT OF A PULSED PLASMA THRUSTER FOR THE ASTER MISSION," *33rd International Electric Propulsion Conference*, 2013.

[6] INPE, "ASTER: The First Brazilian Deep Space Mission - Phase 0," Unpublished, 2012.

[7] J. Fang, J.-L. Margot, M. Brozovic, M. C. Nolan, L. A. Benner, and P. A. Taylor, "Orbits of near-Earth asteroid triples 2001 SN263 and 1994 CC: Properties, origin, and evolution," *The Astronomical Journal*, Vol. 141, No. 5, 2011, p. 154.

[8] G. Gómez, J. Llibre, R. Martínez, and C. Simó, *Dynamics and Mission Design Near Libration Points*, Vol. II Fundamentals: The Case of Triangular Libration Points of *World Scientific Monograph Series in Mathematics*. World Scientific, 2001.

[9] W. Koon, M. W. Lo, J. E. Marsden, and S. D. Ross, *Dynamical Systems, the Three-Body Problem and Space Mission Design*. Marsden Books, 2006.

[10] D. Blazevski and C. Ocampo, "Periodic orbits in the concentric circular restricted four-body problem and their invariant manifolds," *Physica D: Nonlinear Phenomena*, Vol. 241, No. 13, 2012, pp. 1158–1167.

[11] P. Gurfil, *Modern astrodynamics*, Vol. 1. Butterworth-Heinemann, 2006.

[12] O. Montenbruck and E. Gill, *Satellite orbits: models, methods and applications*. Springer Science & Business Media, 2012.

[13] A. Sukhanov, H. d. C. Velho, E. Macau, and O. Winter, "The Aster project: Flight to a near-Earth asteroid," *Cosmic Research*, Vol. 48, No. 5, 2010, pp. 443–450.

[14] M. Giancotti, *Stable Orbits in the Proximity of an Asteroid: Solutions for the Hayabusa 2 Mission*. PhD thesis, Università di Roma, 2014.

[15] S. Kikuchi and Y. Tsuda, "Quasi-periodic orbit design around an asteroid using an impulsive delta-v," *65th International Astronautical Congress*, 2014.

[16] S. Broschart, D. Scheeres, and B. Villac, "New families of multi-revolution terminator orbits near small orbits," *Advances in the Astronautical Sciences*, Vol. 135, 2010, pp. 1685–1702.

[17] S. B. Broschart, G. Lantoine, and D. J. Grebow, "Characteristics of quasi-terminator orbits near primitive bodies," *American Astronomical Society*, 2013.

[18] A. Riaguas, A. Elipe, and M. Lara, "Periodic orbits around a massive straight segment," *Celestial Mechanics and Dynamical Astronomy*, Vol. 73, No. 1-4, 1999, pp. 169–178.

[19] F. Biscani, D. Izzo, and C. H. Yam, "A global optimisation toolbox for massively parallel engineering optimisation," *arXiv preprint arXiv:1004.3824*, 2010.

[20] A. K. Qin and P. N. Suganthan, "Self-adaptive differential evolution algorithm for numerical optimization," *Evolutionary Computation, 2005. The 2005 IEEE Congress on*, Vol. 2, IEEE, 2005, pp. 1785–1791.

[21] J. Brest, V. Zumer, and M. Maucec, "Self-adaptive differential evolution algorithm in constrained real-parameter optimization," *Evolutionary Computation, 2006. CEC 2006. IEEE Congress on*, IEEE, 2006, pp. 215–222.

[22] Q. Zhang and H. Li, "MOEA/D: A multiobjective evolutionary algorithm based on decomposition," *Evolutionary Computation, IEEE Transactions on*, Vol. 11, No. 6, 2007, pp. 712–731.